The influence of low irradiance and electrolytes on the mineralization efficiency of organic pollutants using the Vis-active photocatalytic tandem CuInS$_2$/TiO$_2$/SnO$_2$

Anca Duta *, Luminita Andronic, Alexandru Enesca *

R&D Center Renewable Energy System and Recycling, Transilvania University of Brasov, Eroilor 29 Street, 500036, Brasov, Romania

ARTICLE INFO

ABSTRACT

Many photocatalyitc laboratory experiments are developed at low (and different) irradiance values, making the results difficult to benchmark. This study analyzes the influence of the low irradiance, photon flux and the UV share on the photodegradation kinetics and efficiency of methylene blue (MB) using a hetero-structured thin film photocatalyst. The results show that the photon flux influences the process kinetic after an induction period and it was found that increasing irradiance has positive effect on the photo-catalytic efficiency, if UV does not exceed 25%, when photo-corrosion becomes significant. In the experimental conditions, the efficiency is also moderately influenced by the photon flux vales. Electrolytes are usually part of industrial or residential wastewaters, with multiple consequences among which accelerated photo-corrosion but also increased local charge transfer (thus decreased recombination) on the photocatalytic surface. The addition of two common electrolytes that are not hydrolysing (NaCl and CaCl$_2$) into the dye solution was correlated with the chemical stability of the CIS/TiO$_2$/SnO$_2$ hetero-structure and the removal/mineralization efficiencies. The highest photodegradation efficiency (99%) was reached when 3.5% NaCl was used. The photocorossion increase up to 24.03% after 24 h when the photocatalyst is immersed in 3.5% NaCl electrolyte at 23 W/m^2 UV/vis irradiance and 120 μmol/(m^2 s) photon flux.

1. Introduction

Advanced oxidation processes (AOPs) based on semiconductor photocatalysis have a wide applications range [1–4] as they are recognized to destroy, through mineralization, even very low concentrated pollutants, including the emergent organic pesticides, hormones, antibiotics, etc. Moving to a new or optimised technology based on AOPs implemented in the existing wastewater treatment plants requires to lift the main barriers related to the cost of the m^3 of treated water, variable quality of the effluent and process functionality [4–7]. Among these, the economic factor is by far considered the most relevant as AOPs are energy-intensive, especially due to the most commonly employed UV-activation [8–10]. There are many papers reporting on the use of AOPs based on semiconductors [11–14], composites [15,16] or hybrid [17,18] photocatalysts for the removal of dyes [19–21], phenols [22,23] or drugs

[24,25], but only few of them consider the AOPs feasibility based on energy consumption [26].

Additionally, wastewaters contain many components that are not directly affected by photocatalysis in a process optimised for organic pollutants removal, e.g. the electrolytes. Basically, electrolytes increase the ionic strength in the solution, supporting local charge separation on/near the active sites of the photocatalyst (thus reducing recombination and increasing the overall process efficiency), or may trap reactive oxygen compounds [27,28]; on the other hand, electrolytes may accelerate photo-corrosion or may lead to competitive adsorption with the pollutant on the photocatalytic active sites. The effect of pH (3...9, insured by adding acid or alkaline electrolytes) on photocorrosion was outlined for phenol photodegradation and the pH values close to 7 were found to be the least harmful [29]. However, literature is scarce on data discussing the effect of electrolytes that don't change the pH values (e.g. non-hydrolysable salts) on the photocatalytic processes, although their contribution may be important.

Ultimately, photocatalysis aims at the use of solar radiation, with infield irradiance values of hundreds of W/m^2. However, most of the laboratory experiments are developed at much
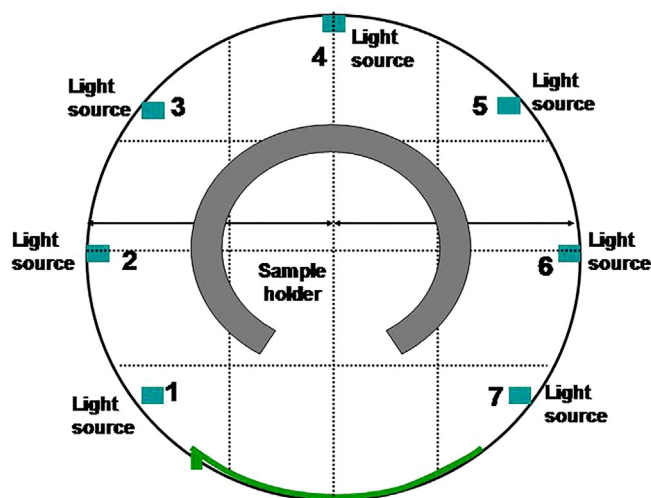
Fig. 1. Top view of the photodegradation setup.

lower (although different) irradiance values, sometimes not even reported. Obviously the input radiation will affect the process kinetics (or mechanisms), making difficult to compare the results; however, literature reports on the influence of low irradiance variation on the photocatalyic process are scarce.

This work discusses the influence of two extrinsic factors on the photocatalytic processes: the effects of low irradiance and of non-hydrolysable salt electrolytes. A p-n-n multi-junction/tandem with the $CuInS_2/TiO_2/SnO_2$ structure is used as photocatalyst and methylene blue (MB) as reference pollutant. The UV/vis share, the photon flux and the irradiance values were varied to investigate the mineralization efficiency. The photocatalyst response in electrolyte media (NaCl and $CaCl_2$) was further investigated, using the irradiation conditions that proved good efficiency and low energy consumption.

2. Experimental procedure

2.1. Photocatalytic materials

The photoactive $CuInS_2/TiO_2/SnO_2$ hetero-structures were obtained by robotic spray pyrolysis deposition (RSPD) using $2 \times 2\,cm^2$ microscopic glasses (Heinz Herenz). The substrate was cleaned by successive immersion in ethanol and acetone, using an ultrasonic bath.

The precursors for the metal oxides layers were prepared by mixing the corresponding salts ($SnCl_4$, 99.99%, Alfa Aesar for SnO_2 and $TiCl_4$, 99.99%, Alfa Aesar for TiO_2 films) with ethanol (C_2H_5OH, 99.99%, Alfa Aesar) to form 0.1 M solutions. The precursor for $CuInS_2$ was obtained from 0.3 M copper chloride ($CuCl_2$, 99%, Scharlau), 0.3 M indium chloride ($InCl_2$, 99.5%, Scharlau) and thiourea ($SC(NH_2)_2$, 99%, Scharlau) in a 1:1.25:4.5 molar ratio, as previously described [30]. The photocatalytic thin films have tetragonal crystalline structures with similar crystallite sizes (82.3 Å for SnO_2, 81.4 Å for TiO_2 and 71.5 Å for $CuInS_2$), well supporting the lattice match.

2.2. The experimental setup

The photodegradation setup consists of a cylindrical aluminium reflective casing having the sample holder centrally positioned; during the experiments, this holds a quartz beaker where the photocatalytic process is employed. On the casing a variable number of 1. . .7 irradiation sources can be vertically mounted, Fig. 1. The

upper part of the casing has controlled air circulation, to avoid temperature increase during the long-term experiments.

The UV irradiation sources were F18W/T8 black light tubes (UVA, typically 340–400 nm, with $\lambda_{UV,\ max} = 365\,nm$, flux intensity 3Lx, Philips), and Vis sources (TL-D Super 80 18W/865 white cold light tubes, typically 400–700 nm, with $\lambda_{Vis,max} = 565\,nm$, flux intensity 28Lx, Philips). Total irradiance values were measured in the central position of the sample holder, using a class A pyranometer (SR11, Hukselflux).

Seven irradiation scenarios using a different number of UV and Vis tubes were implemented. The light sources were placed on different positions on the photo-reactor's casing to obtain a homogeneous distribution of the light on the sample holder (the numbers describing the positions of these light sources in Table 1 correspond to those marked in).

The irradiation scenarios were designed to investigate different aspects of the light conversion during the photocatalysis:

- Scenario 1. . .4: used both UV and Vis light in different ratio and different positions into the photo-reactor;
- Scenario 5 uses the maximum number of Vis sources giving also the maximum irradiance value.
- Scenarios 6 and 7 employ the same irradiance value ($9\,W/m^2$) but use only Vis (6) or only UV (7) sources.

Considering the power of each irradiation source and the number of sources of each type, the share of UV radiation in each experiment was calculated using Eq. (1):

$$UV[\%] = \frac{E_{UV} \cdot n_{UV}}{E_{UV} \cdot n_{UV} + E_{Vis} \cdot n_{Vis}} \cdot 100 \tag{1}$$

On average, the irradiance values corresponding to one single irradiation source, measured on the photoreactor site, were: $E_{UV} = 2.25\,W/m^2$ for the UV, respectively $E_{Vis} = 4.5\,W/m^2$ for the Vis source(s). Based on these values, on the number of sources (n_{UV}, n_{Vis}) and on their maximum emission wavelength ($\lambda_{UV,max}$, $\lambda_{Vis,max}$), the maximum photon flux reaching the quartz beaker during each experimental trial, Φ, was calculated using Eq. (2):

$$\Phi = \frac{E_{UV} \cdot \lambda_{UV} \cdot n_{UV} + E_{Vis} \cdot \lambda_{Vis.} \cdot n_{Vis}}{h \cdot c \cdot N_{Av}} \tag{2}$$

where: the Planck constant (h), the speed of light (c) and the Avogadro number have the usual values.

Details on the irradiation scenarios implemented during the experiments are included in Table 1.

2.3. Photocatalysis experiments

The 0.0125 mM methylene blue (MB, 99.8%, Merck) solution was prepared using ultra-pure water (Direct-Q3 Water Purification System).

First group of experiments were run to investigate the effect of the irradiance/photon flux on the photocatalytic process involving the thin film hetero-structure and the MB blue solution.

Second group of experiments: following the results, two irradiation scenarios were selected to further investigate the electrolytes influence; experiments were run using 0.0125 mM methylene blue solutions with NaCl and, respectively $CaCl_2$ added to get two concentrations (1% and 3.5%) in the photocatalytic system.

Before irradiation, each thin film sample was inserted in 30 mL dye solution into the quartz beaker and kept in dark for 2 h to reach the adsorption/desorption equilibrium. Hourly measured data were initially employed, up to 6 h of photocatalysis. Long term stability tests were further conducted in three cycles of 8 h each.

The MB removal efficiency was assessed based on the changes in concentration evidenced on the absorption calibration curve